Rayleigh-normalized Gaussian Noise in Blind Signal Fusion

Aaron Ballew
ballew@u.northwestern.edu

Aleksandar Kuzmanovic
akuzma@northwestern.edu

Chung Chieh Lee
cclee@northwestern.edu

***Abstract*—This paper builds upon a previously defined fusion process that exploits multichannel receiver diversity to enhance received SNR. This particular diversity combiner aims to enhance SNR under the challenging constraints that channel gains are unknown, there is no direct knowledge of the transmitted signal, and no opportunity to precode the signal into a known waveform. Thus, fusion is blind in the sense that indirect techniques are invoked to intelligently weight each sample during fusion, and to measure the outcome.**

Having already established a critical threshold that determines whether fusion does or does not enhance SNR, this paper takes the next step by pursuing rigorous analytical development of a statistical noise model for the effects of the combiner. We provide the probability distributions of this noise, termed Rayleigh-normalized Gaussian. With the probability distributions in hand, we apply them to sample sets of various sizes to understand how the combiner behaves with each incremental sample. This allows us to investigate the likelihood that the critical threshold for SNR gain is met, relative to additional samples, as well as the likelihood of meeting arbitrary target SNR gains. We also develop an expression for the average power of the Rayleigh-normalized Gaussian noise variable.

I. Introduction

In [1], a diversity combiner is described that addresses a scenario in which many noise-corrupted copies of a source signal are to be fused for the purpose of increasing signal to noise ratio (SNR) over any single received copy. This is to be achieved under the challenging constraints that channel gains are unknown, there is no direct knowledge of the transmitted signal, and no opportunity to precode the signal into a known waveform. Thus, many techniques common to digital communications that exploit pilot signals, digital encoding (M-ary QPSK/QAM), or those that invoke channel gain (MRC [2]) are not applicable. The received signals are analog in nature, even if stored digitally. Thus, fusion is blind in the sense that indirect techniques must be applied to intelligently weight each sample during fusion, and to measure the outcome of the process.

Though clearly approached from a communications point of view, the combiner's original motivation comes from a real-world example in which numerous recordings of a single musical performance are captured by audience members and shared online. Signal generated from stage-speakers is recorded in mono by arbitrarily distributed receivers, a common practice enabled by mobile phones and digital cameras. The noise captured at each receiver differs among the recordings due to spatial diversity that can be exploited during combining.

In the prior work, a critical threshold (detailed in Section II, Eq. 1) was identified that defines whether the outcome of fusion does or does not enhance SNR over any original received sample. This model requires only that noise is uncorrelated, and assumed no particular statistical distribution on the noise. Now we wish to deepen our understanding of the combiner by investigating not only whether fusion is successful, but how likely it is to be successful for sample sets of varying size. In order to accomplish such a characterization, it is necessary to assume a distribution on the noise, which will allow us to calculate probabilities associated with various input conditions.

In this paper, we make reasonable assumptions on noise, and through the effects of the combiner identify a new noise random variable, termed Rayleigh-normalized Gaussian (RnG). We pursue rigorous analytical development of the closed-form probability density functions (PDF) for both noise amplitude and power. With the PDFs in hand, we apply them to sample sets of various sizes to understand how the combiner behaves with each incremental sample. It should be emphasized that our goal here is not to build exhaustive tables of probabilities (since any particular probability value depends on many parameters), but rather to understand the trending behavior of the combiner. The paper is organized into three main sections. Section II gives brief but important background on the fusion process that motivates the subsequent analysis, Section III presents the closed-form distributions, and Section IV provides evaluation and further discussion of the results.

II. Normalized Gain Combining Background

The combiner, here termed Normalized Gain Combining (NGC), relies on the following observation: When adding uncorrelated noise of differing powers to identical transmitted signals, the differences in total powers among the received sample signals is due to noise. Therefore, NGC attempts to normalize received samples such that their component signal powers, rather than noise or total powers, are equal.

Meeting this condition allows NGC to rank all noisy samples in a set by relative SNR and judge whether a fused sample returns increased or decreased SNR, all without knowing explicitly the SNR of any individual or fused sample. The critical enabling detail is the assurance that the powers from the source signal components of each of the noisy samples are equal. Note that the condition of equal powers does not imply knowledge of what that power actually is, hence the absolute SNRs remain unknown.

To understand how this normalization is achieved, let N be the number of available received samples, x_i, where $i, j = 1, 2 \ldots N$. i and j are indices used to distinguish between two samples x_i being simultaneously considered, though $i = j$ is permitted. Assume all x_i in the set are already synchronized, a procedure addressed in [1], but beyond the scope of

this discussion. Assume noise is uncorrelated (this is more precisely defined in a moment). Then, let $\text{Cov}(x_{\text{ref}}, x_i) = c_i$, and $\text{Cov}(x_{\text{ref}}, x_j) = c_j$. Then $\text{Cov}(x_{\text{ref}}, x_i) = c_i \equiv h_j \cdot c_j = \text{Cov}(x_{\text{ref}}, h_j x_j)$, where h_j, c_j, and c_i are constants, and x_{ref} is any fixed sample from the set chosen as an internal reference. Cov represents covariance. Thus there is a scaling factor h_j which sets equal the covariances of any two samples to a third sample. By applying this technique repeatedly throughout the sample set, all samples can be scaled such that their covariances to x_{ref} are equal. In a final pass x_{ref} can relinquish its role as the internal reference to another sample in the set, and similarly be scaled to set its covariance to that new reference equal with the remaining samples' covariance to that new reference. Upon conclusion of this procedure, powers from the source signal are equal (though it remains unknown what the absolute power is), and differences in total powers among the normalized samples are due to the noise.

This allows for ranking of the normalized samples in order of increasing noise power, relabeling the sample with lowest power x_1. Taking the average of the normalized samples results in a fused output with unchanged signal power, and total power that is either increased or decreased. If the total power is lower than that of x_1, then based on our assumptions, fusion has resulted in an increase in SNR.

Assume a set of normalized samples ranked in order of increasing noise power, in which the noise power is known. Let k_i, for $i = 1, 2 \ldots N$, be the ratio of the i^{th} ranked sample's noise power to the 1st ranked (i.e., the "best" of those received) sample's noise power. Then, $k_1 = 1$, and it can be shown [1] that post-fusion SNR improvement is achieved when there exists a subset M that satisfies the following condition:

$$\frac{M^2}{\sum_{i=1}^{M} k_i} > 1, \quad 1 \leq M \leq N \tag{1}$$

M indicates that it may be necessary to fuse only a subset of the N ranked samples in order to achieve SNR gain. This can happen, for example, when the poorest samples contribute so much noise power and so little signal power that any noise-cancellation effect is overwhelmed.

III. Analysis

Noting that Eq. 1 makes no assumption on the noise distribution, other than being uncorrelated, we now shift our attention to understanding the likelihood that Eq. 1 can be met. This requires a noise model that will serve as the basis for the remainder of this paper.

Let s_i be the faded form of the original transmitted signal s. Let $n_i \sim G(0, \sigma_{n_i}^2)$ be uncorrelated Gaussian noise, such that $\text{Cov}(n_i, n_j) = 0$, $i \neq j$ and $\text{Cov}(s_i, n_i) = 0$, $\forall i$. Let $a_i \sim R(\sigma_{a_i}^2)$ be a Rayleigh distributed scaling factor, and $s_i = a_i s$. Then $x_i = a_i s + n_i$ and $\sigma_{x_i}^2 = a_i^2 \sigma_s^2 + \sigma_{n_i}^2$.

The choice of Rayleigh distributed fading for a_i deserves special consideration. Rayleigh fading is a powerful model commonly applied in multichannel systems [2], [3], [4] when line-of-sight is compromised, or when spatial diversity [5], [6] is present including multiantenna MIMO [7] and even vehicular networks [8], [9]. In the present context, our motivating scenario assumes that recordings come from users that are arbitrarily dispersed among the audience, supplying spatial diversity. In practice our observation is that received samples do exhibit differing levels of loudness relative to background noise. We consider Rayleigh fading a reasonable starting point for analysis, that may later be refined.

Given $x_i = a_i s + n_i$, consider a set of normalized ranked samples. For purposes of notational convenience and without loss of generality, assume that normalization successfully sets signal power s_i in each sample equal to that of the original transmitted signal s, by essentially *dividing out* a_i. Then, $x_i' = x_i / a_i = s + n_i / a_i$. Let $n_i / a_i \equiv v_i$, the newly defined RnG noise term collecting both the Gaussian and Rayleigh components.

In practice, NGC normalizes relative to the power of an internal reference chosen from the set of received samples, not the power of the original transmitted signal s. For example, in the case that all received samples are normalized to the power of $a_1 s$, then $v_i = n_i / (a_i / a_1)$, $\forall i$. Dividing the various a_i by the same a_1 is equivalent to dividing a Rayleigh distributed random variable by a constant, and the resulting $a_i' = a_i / a_1$ is still Rayleigh distributed.

We now present the closed-form RnG distributions. Detailed derivations can be found in the Appendix, Section VI.

A. RnG Amplitude

The following are the CDF and PDF of the RnG random variable v_i, with $n_i \sim G(0, \sigma_{n_i}^2)$, and $a_i \sim R(\sigma_{a_i}^2)$. The CDF and PDF are first derived with limits inherited from the standard Gaussian and Rayleigh distributions, namely $(-\infty, \infty)$ and $(0, \infty)$, respectively. They are then rederived and generalized with truncation of the Rayleigh component that directly maps to a critical aspect of the NGC algorithm. Truncation enables an important guarantee that σ_{v^2}, or RnG average power, is finite. The subscript i is dropped since v_i are i.i.d.

1) CDF:

$$F_v(x) = P(v \leq x) = P\left(\frac{n}{a} \leq x\right) \tag{2}$$

$$= \int_0^\infty \Phi\left(\frac{ax}{\sigma_n}\right) f(a) da \tag{3}$$

$$= \frac{1}{2}\left[1 + x\sqrt{\frac{\sigma_a^2}{\sigma_n^2 + x^2\sigma_a^2}}\right] \tag{4}$$

where $\Phi(\cdot)$ is the unit Gaussian CDF, and $f(a)$ is the Rayleigh PDF with $a > 0$, thus the limits of 0 to ∞. The CDF of v, $F_v(x)$, is shown in Fig. 1 for different values of σ_a^2 and σ_n^2.

2) PDF:

$$f_v(x) = \frac{d}{dx} F_v(x) \tag{5}$$

$$= \frac{\sigma_a \sigma_n^2}{2\left(\sigma_n^2 + x^2\sigma_a^2\right)^{\frac{3}{2}}} \tag{6}$$

The PDF of v, $f_v(x)$, follows from the derivative of the CDF and is shown in Fig. 2 for different values of σ_a^2 and

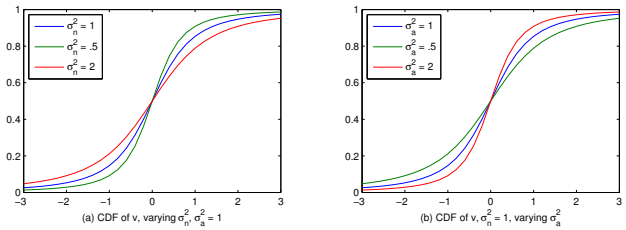

Fig. 1. $F_v(x)$, the CDF of RnG noise amplitude

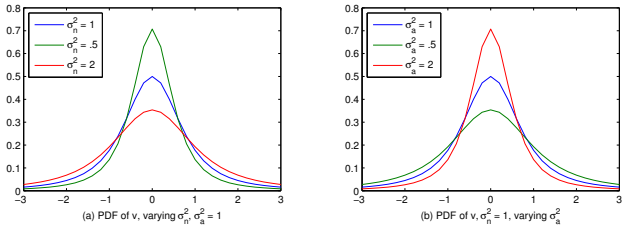

Fig. 2. $f_v(x)$, the PDF of RnG noise amplitude

σ_n^2. It can be shown that the decay of the PDF is too slow to ensure a finite σ_{v^2}, an issue resolved in the next section.

3) CDF with Truncation: Intuitively, noise of the form "n over a" leads us to expect an increase in overall noise v whenever a is small. Signals with small a are deeply faded and can result in an exploding RnG noise v. The NGC algorithm eliminates very noisy signals that cannot contribute to an improved fusion output. To represent this behavior, we place a lower limit α on the Rayleigh random variable a. Though there need not be a limit on how strong a signal can be, NGC by design also identifies the best received signal, so we place an upper limit β on a. These limits thus correspond directly to the behavior of the NGC algorithm, and allow redevelopment of generalized RnG distributions such that σ_{v^2} must be finite. The following presents truncated $F_v(x)$, where $0 < \alpha \leq a \leq \beta$.

$$F_v(x) = \int_\alpha^\beta \Phi\left(\frac{ax}{\sigma_n}\right) f_{\alpha,\beta}(a)da \tag{7}$$

$$= \frac{1}{e^{\frac{-\alpha^2}{2\sigma_a^2}} - e^{\frac{-\beta^2}{2\sigma_a^2}}} \left[\Phi\left(\frac{\alpha x}{\sigma_n}\right) e^{\frac{-\alpha^2}{2\sigma_a^2}} - \Phi\left(\frac{\beta x}{\sigma_n}\right) e^{\frac{-\beta^2}{2\sigma_a^2}} + \int_\alpha^\beta \frac{x}{\sqrt{2\pi\sigma_n^2}} \; e^{\frac{-a^2}{2\left[\frac{\sigma_a\sigma_n}{\sqrt{\sigma_n^2+x^2\sigma_a^2}}\right]^2}} da \right] \tag{8}$$

where $\Phi(\cdot)$ is the unit Gaussian CDF, and $f_{\alpha,\beta}(a)$ represents the truncated Rayleigh PDF,

$$f_{\alpha,\beta}(a) = \frac{1}{F(\beta) - F(\alpha)} \cdot \frac{a}{\sigma_a^2} \; e^{\frac{-a^2}{2\sigma_a^2}} \tag{9}$$

$$= \frac{1}{e^{\frac{-\alpha^2}{2\sigma_a^2}} - e^{\frac{-\beta^2}{2\sigma_a^2}}} \cdot \frac{a}{\sigma_a^2} \; e^{\frac{-a^2}{2\sigma_a^2}} \tag{10}$$

4) PDF with Truncation: The PDF of truncated $f_v(x)$ again follows from the derivative of the CDF.

$$f_v(x) = \frac{1}{e^{\frac{-\alpha^2}{2\sigma_a^2}} - e^{\frac{-\beta^2}{2\sigma_a^2}}} \left[\frac{\sigma_n}{\sqrt{2\pi}(\sigma_n^2 + x^2\sigma_a^2)} \left(\alpha e^{\frac{-\alpha^2}{2\sigma^2}} - \beta e^{\frac{-\beta^2}{2\sigma^2}} \right) + \frac{\sigma_a\sigma_n^2}{(\sigma_n^2 + x^2\sigma_a^2)^{\frac{3}{2}}} \left[\Phi\left(\frac{\beta}{\sigma}\right) - \Phi\left(\frac{\alpha}{\sigma}\right) \right] \right] \tag{11}$$

where $\sigma \equiv \frac{\sigma_a\sigma_n}{\sqrt{\sigma_n^2+x^2\sigma_a^2}}$ for compactness. Setting $\alpha = 0$ and $\beta = \infty$, Eq. 11 reduces to Eq. 6.

B. RnG Power

Already having the PDF of v, the PDF of truncated v^2 is included here for completeness. In addition, we are interested in the average RnG noise power, σ_v^2. Let $\sigma_v^2 = E[v^2] - E[v]^2$. We know Eq. 11 gives the density of truncated v, and Fig. 2 illustrates that $E[v] = 0$ (which is intuitive due to the symmetry of the Gaussian density function). This allows us to focus on $E[v^2]$ when characterizing the average noise power of an RnG random variable. The following presents truncated $f_{v^2}(x)$ and $E[v^2]$ as a function of α, β.

1) PDF with Truncation:

$$f_{v^2}(x) = \frac{1}{|x|} \cdot \frac{1}{e^{\frac{-\alpha^2}{2\sigma_a^2}} - e^{\frac{-\beta^2}{2\sigma_a^2}}} \cdot \left[\frac{\sigma_n}{\sqrt{2\pi}(\sigma_n^2 + x^2\sigma_a^2)} \left(\alpha e^{\frac{-\alpha^2}{2\sigma^2}} - \beta e^{\frac{-\beta^2}{2\sigma^2}} \right) + \frac{\sigma_a\sigma_n^2}{(\sigma_n^2 + x^2\sigma_a^2)^{\frac{3}{2}}} \left[\Phi\left(\frac{\beta}{\sigma}\right) - \Phi\left(\frac{\alpha}{\sigma}\right) \right] \right] \tag{12}$$

where $\sigma \equiv \frac{\sigma_a\sigma_n}{\sqrt{\sigma_n^2+x^2\sigma_a^2}}$ for compactness.

2) Average Power: Truncation guarantees that the noise amplitude lies within the range $\frac{\sigma_n}{\beta} \leq v \leq \frac{\sigma_n}{\alpha}$, for $0 < \alpha \leq a \leq \beta$, even without knowledge of the density. Truncation also guarantees the expected value of the noise power, $\sigma_{v^2} = E[v^2]$, is finite.

To find $E[v^2]$, recall that $v = \frac{n}{a}$ and $v^2 = \frac{n^2}{a^2}$.

$$E[v^2] = E\left[\frac{n^2}{a^2}\right] = E[n^2] \cdot E\left[\frac{1}{a^2}\right] \tag{13}$$

$$= \sigma_n^2 \cdot \int_\alpha^\beta \frac{1}{a^2} \frac{a}{\sigma_a^2} e^{\frac{-a^2}{2\sigma_a^2}} da \tag{14}$$

$$= \frac{\sigma_n^2}{2\sigma_a^2} \left[Ei\left(-\frac{\beta^2}{2\sigma_a^2}\right) - Ei\left(-\frac{\alpha^2}{2\sigma_a^2}\right) \right] \tag{15}$$

where the Exponential Integral [10] is represented by $Ei(z) = \int_{-\infty}^{z} \frac{e^t}{t} dt$, and $\int \frac{e^{-cx^2}}{x} dx = \frac{1}{2} Ei(-cx^2)$. For $0 < \alpha \leq a \leq \beta$, $E[v^2] < \infty$. Fig. 3 illustrates the relationship among $E[v^2]$, α, and β, and its intuitive correspondence to the "n over a" form of v. As α shrinks, $E[v^2]$ grows. If α were allowed to shrink unbounded toward 0, $E[v^2]$ would grow to infinity.

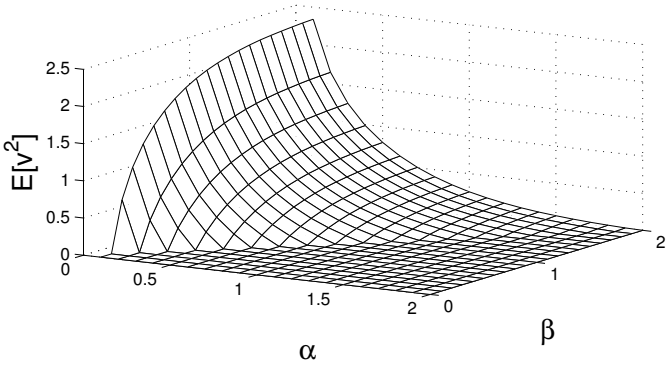

Fig. 3. Average Power $E[v^2]$ vs. α and β

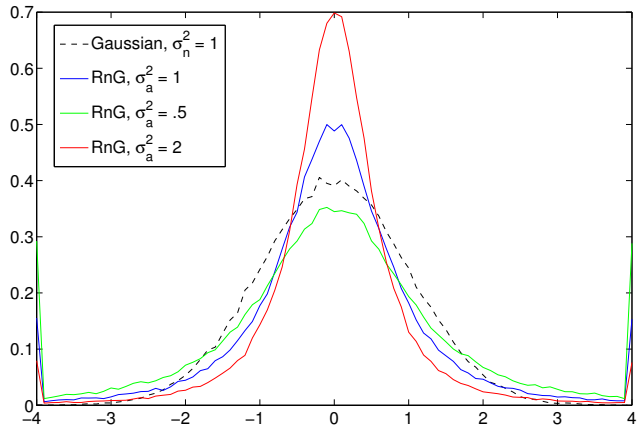

Fig. 4. $f_v(x)$, the PDF of RnG noise amplitude, generated via simulation of Gaussian and Rayleigh distributed data points, for varying σ_a^2. For added context, a Gaussian-only density with $\sigma_n^2 = 1$ is superimposed.

IV. Evaluation

In this section, we apply the results of our analysis to better understand the marginal behavior of fusion via NGC, i.e., the incremental effect of increasing the size of the sample set.

As pointed out in Section III-B2, Fig. 3 illustrates that $E[v^2]$ exhibits an intuitive correspondence to the "n over a" form of v. Similarly, the density plots of Fig. 2 fall in line with expectations. Since Gaussian random variables have symmetry (assuming zero-mean) in that they take positive and negative values, multiplying or dividing by a Rayleigh random variable that can take only positive values implies symmetry will be preserved in RnG noise. However, we expect the density to be stretched or compressed due to the Rayleigh scaling influence. This is exactly what is observed in Fig. 2.

To further validate the analytical result depicted in Fig. 2, we have generated a simulation of RnG noise and plotted its density in Fig. 4. For added context and ease of comparison, the PDF of a Gaussian-only simulation has also been superimposed over the RnG density. Comparing Figs. 2(b) and 4, there is direct agreement that persists even when varying σ_a^2. These two figures plot the same information in the same way, with the only difference being whether the data was produced via analysis or simulation.

In order to understand how to apply the RnG PDF, we revisit Eq. 1. Recall that the threshold $M^2/\sum_{i=1}^{M} k_i > 1$ represents the condition under which SNR in the fused output exceeds that of the 1st-ranked original sample. This condition exists independently of any distribution. It depends only on the number of fused samples, M, and the disparity among noise powers in the sample set as indicated by the ratios k_i. The reason for considering the disparity among noise powers is one of arithmetic. When averaging two uncorrelated noise signals of equal powers, noise cancellation results in a fused output with less power than either of the original noise signals. When one noise signal's power is much greater than the other's, averaging still results in a degree of cancellation, but the power of the fused output may actually exceed that of the lower-powered of the original noise signals. In that case, fusion provided no benefit and the lower-powered original noise signal should be preferred. Somewhere between these examples is a point where noise cancellation and noise disparity exactly balance, such that the fused output has noise power exactly equal to that of the lower-powered of the original noise signals. That balance point arises when $M^2 = \sum_{i=1}^{M} k_i$.

Fig. 5 examines the relationship among M^2, $\sum_{i=1}^{M} k_i$, and SNR gain from fusion, for an illustrative realization. In this realization, all k_i, $i = 2 : M$, are set equal to each other. With the exception of $k_1 = 1$, the particular value chosen is $E[v^2]$ as calculated by Eq. 15 ($k_1 = 1$ offers the convenience that the ratios k_i are the noise powers themselves). In Fig. 5(top), M^2 is seen growing rapidly with M, while $\sum_{i=1}^{M} k_i$ does not. With so many of the k_i set equal, this is a very favorable condition to SNR gain, and this is visible in Fig. 5(bottom). However, by introducing noise power disparity between k_1 and the other samples, an important characteristic emerges. A highly-ranked subset of the ranked samples may be unable to meet the threshold for improved SNR, and by including more samples, the threshold may then become satisfied. This is seen in Fig. 5(bottom), where SNR improvement relative to the best sample is not achieved for $M = 2$ and $M = 3$. Only when $M \geq 4$ is SNR enhanced. For this reason, it is necessary to fuse every subset of the first-M ranked samples (i.e., the first two, the first three, the first four, etc.) out of the total N available samples prior to determining which subset provides optimal SNR gain. Note that ranking provides the valuable computational advantage of limiting the number of test subsets to N, eliminating the need to test every combination within the N total samples. Given this behavior, it is of great interest to investigate the effect each incremental sample is likely to have when being added to the fused subset. More precisely, we describe this as the marginal effect of the M^{th} sample, given an existing realization of the first $M-1$ samples.

To study the M^{th} sample, we will isolate it according to Eq. 20. Based on an assumed realization of $k_1 : k_{M-1}$, and the corresponding $\sum_{i=1}^{M-1} k_i$, we can calculate what value of k_M is necessary in order to satisfy the threshold of Eq. 1. This critical value then serves as the input argument of Eq. 12, the PDF of v^2. Equivalently, $\sqrt{k_M}$ as shown in Eq. 20 serves as the input for Eq. 11, the PDF of v. The result is the probability that the incremental addition of k_M to the set

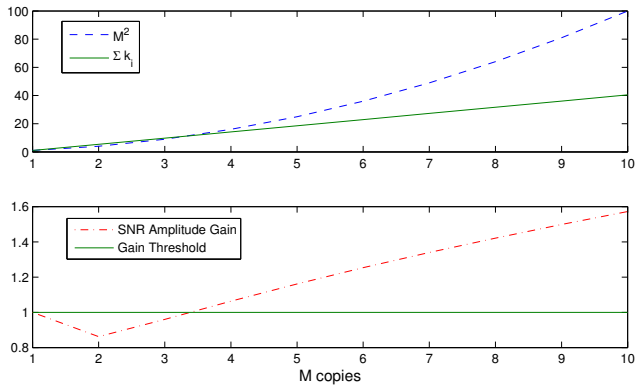

Fig. 5. Plot of M^2, $\sum_{i=1}^{M} k_i$, and SNR Amplitude Gain vs. M samples. Assume $k_1 = 1$, $k_2 : k_M = E[v^2]$ for $\sigma_n^2 = \sigma_a^2 = \beta = 1$, $\alpha = 0.01$

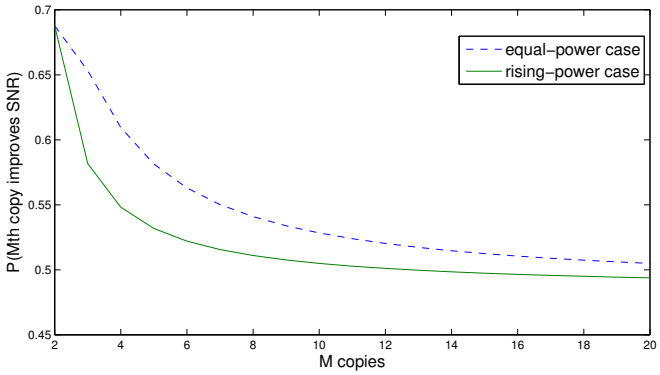

Fig. 6. Plot of truncated $F_v(x = \left|\sqrt{k_M}\right|)$ vs. M, where $\sqrt{k_M}$ is determined by the maximum allowable RnG noise in the M^{th} sample that will allow for improved SNR after fusion. Assume $\sigma_n^2 = \sigma_a^2 = 1, \alpha = 0$

will result in improved SNR due to fusion. As a matter of preference, we will proceed focusing on $\sqrt{k_M}$ and truncated $f_v(x)$ in the amplitude domain.

$$\frac{M^2}{\sum_{i=1}^{M} k_i} > 1 \tag{16}$$

$$M^2 > \sum_{i=1}^{M} k_i \tag{17}$$

$$M^2 > \sum_{i=1}^{M-1} k_i + k_M \tag{18}$$

$$M^2 - \sum_{i=1}^{M-1} k_i > k_M \tag{19}$$

$$\sqrt{M^2 - \sum_{i=1}^{M-1} k_i} > \sqrt{k_M} \tag{20}$$

The next consideration is what realization to assume for the first $k_1 : k_{M-1}$ ranked samples. There are two realizations in particular that are highly instructive. The first has already been hinted at, and that is the advantageous case when all noise powers are equal, or $k_i = 1$, $\forall i$. The second is a less favorable case in which noise disparity is introduced to the sample set, so much so that the growth in $\sum_{i=1}^{M-1} k_i$ exactly keeps pace with $(M-1)^2$ as M increases. This growth rate in noise power prevents improved SNR from fusion of the first $M-1$ samples while ensuring it is still possible through addition of the M^{th}. Such a realization can be generated by setting $k_i = 2i - 1$. Observe the following realization of a sequence of k_i, [1 3 5 7]. It is apparent that $\sum_{i=1}^{2} k_i = 4$, $\sum_{i=1}^{3} k_i = 9$, and $\sum_{i=1}^{4} k_i = 16$, exactly matching the square of the number of samples in the sum.

These two realizations of $k_1 : k_{M-1}$, the equal-power and rising-power cases, respectively, are the basis for Fig. 6. In Fig. 6, each data point is the result of assuming the previously described realizations of the first $M-1$ samples, calculating the necessary $\sqrt{k_M}$ in the M^{th} sample that would meet the threshold set in Eq. 20, and using that result as the input of Eq. 11, truncated $f_v(x)$. The Rayleigh amplitude bound β is chosen in each case such that the M^{th} sample cannot surpass the SNR of the $(M-1)^{th}$ sample, preserving rank. We set $\alpha = 0$ to allow the M^{th} sample to be arbitrarily bad.

Several observations can be made from Fig. 6. In both cases, the highest ranked samples have a high probability of contributing favorably towards improved SNR. As expected, the equal-power case offers a lower hurdle for each M^{th} sample to overcome. In the rising-power case, each M^{th} sample has a smaller range of permissible a, by virtue of having been ranked lower than sample $M-1$. However, in both cases, diminishing returns come into play. Probabilities plunge such that the curves tend to converge beyond approximately 10 samples. Note that the specific probabilities of the y-axis should not cause undue distraction. These values change for different input paramters σ_n^2 and σ_a^2. The curves shift upward or downward, but the general shape persists.

Returning to the example in which many audio recordings of the same event have been shared online, our real-world observation is that 3 to 6 copies is typical, with the number rarely exceeding 10. In this application of NGC, the plausible range of operation occupies the area of the curve in which there is a strong probability of SNR improvement due to fusion.

An additional investigation into applying truncated $f_v(x)$ is shown in Fig. 7. In this example, the size of the sample set is held at $M = 6$. Given an assumed equal-power realization of the first $M-1$ samples, $k_1 : k_5 = 1$, the likelihood that k_6 enables a targeted SNR amplitude gain due to fusion is calculated and plotted. This plot indicates an approximately linear decay in probability, and exact values are again dependent on the choice of input parameters σ_n^2, σ_a^2, α, and β.

In summary, an understanding of fusion via NGC depends on characterizing the impact each incremental sample has when added to the set. To illustrate that impact, we incorporate knowledge of the condition under which SNR improvement is achieved with knowledge of the statistical distribution of RnG noise. This enables us to visualize the marginal effects for any combination of input parameters, including M, σ_n^2, σ_a^2, α, and β.

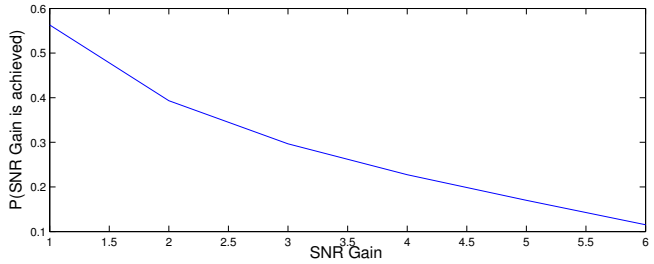

Fig. 7. Plot of truncated $F_v(x = \left|\sqrt{k_M}\right|)$ vs. SNR Amplitude Gain, where $\sqrt{k_M}$ is determined by the maximum allowable RnG noise in the M^{th} sample that will allow for a target SNR Gain after fusion. Assume $\sigma_n^2 = \sigma_a^2 = 1, \alpha = 0$, $M = 6$

V. Conclusion

We have rigorously analyzed Rayleigh-normalized Gaussian noise in the context of an audio signal combiner. By providing densities, expectation of power, and describing their intuitive relation to this form of noise, it is possible to understand the marginal effect of an increasing number of samples available for fusion.

We have provided background on the algorithmic operation of Normalized Gain Combining, which directly motivates Rayleigh-normalized Gaussian noise. In the process of developing the RnG densities, we accommodated the need to ensure finite average noise power. This was accomplished by placing bounds on the Rayleigh amplitude, which itself offers three benefits. Average noise power is ensured to be finite, the bounds map directly to a key feature of the combiner, and the densities become more generalized and thus more powerful.

We then provided several visualizations of our results, including a density for simulated RnG noise that adheres closely to the analytically-derived density. Marginal impact from the incremental addition of samples to the set was shown to have a high probability of supporting SNR gain for the first several samples, with diminishing returns beyond approximately 10 samples. This implies that seeking large sample sets beyond 10 samples provides little incremental value, when the most beneficial samples have already been incorporated.

Above all, this work demonstrates the behavior of a unique blind fusion process that operates under challenging constraints. The absence of channel gains and reference information about the transmitted signal were overcome using indirect methods from statistical signal processing and information fusion, and in the process a new form of noise was identified and studied.

VI. Appendix

In the interest of preserving readability, derivations are kept to a minimum in the body of this paper. In this appendix, detailed derivations are presented for a selection of the more involved solutions. These are: truncated CDF of v, truncated PDF of v, and truncated PDF of v^2.

A. CDF of v with Truncation

Note the truncated Rayleigh PDF,

$$f_{\alpha,\beta}(a) = \frac{1}{F(\beta) - F(\alpha)} \cdot \frac{a}{\sigma_a^2}\, e^{\frac{-a^2}{2\sigma_a^2}} \tag{21}$$

$$= \frac{1}{e^{\frac{-\alpha^2}{2\sigma_a^2}} - e^{\frac{-\beta^2}{2\sigma_a^2}}} \cdot \frac{a}{\sigma_a^2}\, e^{\frac{-a^2}{2\sigma_a^2}} \tag{22}$$

Then substituting below, and integrating by parts gives the truncated $F_v(x)$ in Eq. 26.

$$F_v(x) = P(v \le x) = P\left(\frac{n}{a} \le x\right) \tag{23}$$

$$= \int_\alpha^\beta \Phi\left(\frac{ax}{\sigma_n}\right) f_{\alpha,\beta}(a)da \tag{24}$$

$$= \left[\Phi\left(\frac{ax}{\sigma_n}\right) \frac{-1}{e^{\frac{-\alpha^2}{2\sigma_a^2}} - e^{\frac{-\beta^2}{2\sigma_a^2}}}\, e^{\frac{-a^2}{2\sigma_a^2}}\right]_\alpha^\beta \tag{25}$$

$$- \int_\alpha^\beta \frac{-1}{e^{\frac{-\alpha^2}{2\sigma_a^2}} - e^{\frac{-\beta^2}{2\sigma_a^2}}}\, e^{\frac{-a^2}{2\sigma_a^2}} \frac{x}{\sqrt{2\pi\sigma_n^2}}\, e^{\frac{-(ax)^2}{2\sigma_n^2}} da$$

$$= \frac{1}{e^{\frac{-\alpha^2}{2\sigma_a^2}} - e^{\frac{-\beta^2}{2\sigma_a^2}}} \left[\Phi\left(\frac{\alpha x}{\sigma_n}\right) e^{\frac{-\alpha^2}{2\sigma_a^2}} - \Phi\left(\frac{\beta x}{\sigma_n}\right) e^{\frac{-\beta^2}{2\sigma_a^2}} + \int_\alpha^\beta \frac{x}{\sqrt{2\pi\sigma_n^2}}\, e^{2\left[\frac{\sigma_a\sigma_n}{\sqrt{\sigma_n^2 + x^2\sigma_a^2}}\right]^2} da\right] \tag{26}$$

B. PDF of v with Truncation

The PDF of truncated $f_v(x)$ again follows from the derivative of the CDF. For manageability during the calculation of its derivative, separate $F_v(x)$ into sections J, $K(x)$, and $L(x)$, such that $F_v(x) = J(K(x) + L(x))$, as follows,

$$J \equiv \frac{1}{e^{\frac{-\alpha^2}{2\sigma_a^2}} - e^{\frac{-\beta^2}{2\sigma_a^2}}} \tag{27}$$

$$K(x) \equiv \Phi\left(\frac{\alpha x}{\sigma_n}\right) e^{\frac{-\alpha^2}{2\sigma_a^2}} - \Phi\left(\frac{\beta x}{\sigma_n}\right) e^{\frac{-\beta^2}{2\sigma_a^2}} \tag{28}$$

$$L(x) \equiv \int_\alpha^\beta \frac{x}{\sqrt{2\pi\sigma_n^2}}\, e^{2\left[\frac{\sigma_a\sigma_n}{\sqrt{\sigma_n^2 + x^2\sigma_a^2}}\right]^2} da \tag{29}$$

Then $f_v(x) = \frac{d}{dx}J(K(x)+L(x)) = J(\frac{d}{dx}K(x)+\frac{d}{dx}L(x))$. This allows us to focus on each smaller component of the whole, starting with $\frac{d}{dx}K(x)$ (note J requires no differentiation as it is not a function of x).

$$\frac{d}{dx}K(x)= \frac{d}{dx}\left[\Phi\left(\frac{\alpha x}{\sigma_n}\right)e^{\frac{-\alpha^2}{2\sigma_a^2}}-\Phi\left(\frac{\beta x}{\sigma_n}\right)e^{\frac{-\beta^2}{2\sigma_a^2}}\right] \tag{30}$$

$$= \frac{\alpha}{\sqrt{2\pi}\sigma_n}e^{\frac{-\alpha^2}{2\left[\frac{\sigma_a\sigma_n}{\sqrt{\sigma_n^2+x^2\sigma_a^2}}\right]^2}}-\frac{\beta}{\sqrt{2\pi}\sigma_n}e^{\frac{-\beta^2}{2\left[\frac{\sigma_a\sigma_n}{\sqrt{\sigma_n^2+x^2\sigma_a^2}}\right]^2}} \tag{31}$$

$$= \frac{\alpha}{\sqrt{2\pi}\sigma_n}\ e^{\frac{-\alpha^2}{2\sigma^2}}-\frac{\beta}{\sqrt{2\pi}\sigma_n}\ e^{\frac{-\beta^2}{2\sigma^2}} \tag{32}$$

where $\sigma \equiv \frac{\sigma_a\sigma_n}{\sqrt{\sigma_n^2+x^2\sigma_a^2}}$ for compactness . Now continuing with $\frac{d}{dx}L(x)$, substituting $\sigma \equiv \frac{\sigma_a\sigma_n}{\sqrt{\sigma_n^2+x^2\sigma_a^2}}$, and invoking Leibniz's Rule for differentiation inside an integral [11], we have,

$$\frac{d}{dx}L(x)= \int_\alpha^\beta \frac{d}{dx}\frac{x}{\sqrt{2\pi\sigma_n^2}}\ e^{\frac{-a^2}{2\sigma^2}}da \tag{33}$$

$$= \frac{\sigma}{\sigma_n}\int_\alpha^\beta \frac{1}{\sqrt{2\pi}\sigma}\ e^{\frac{-a^2}{2\sigma^2}}da-\frac{x^2}{\sigma_n^3}\int_\alpha^\beta \frac{a^2}{\sqrt{2\pi}}\ e^{\frac{-a^2}{2\sigma^2}}da \tag{34}$$

$$= \frac{\sigma}{\sigma_n}\left[\Phi\left(\frac{\beta}{\sigma}\right)-\Phi\left(\frac{\alpha}{\sigma}\right)\right] -\frac{x^2}{\sigma_n^3}\left[\frac{\alpha\sigma^2}{\sqrt{2\pi}}e^{\frac{-\alpha^2}{2\sigma^2}}-\frac{\beta\sigma^2}{\sqrt{2\pi}}e^{\frac{-\beta^2}{2\sigma^2}}+\sigma^3\Phi\left(\frac{\beta}{\sigma}\right)-\sigma^3\Phi\left(\frac{\alpha}{\sigma}\right)\right] \tag{35}$$

Recombining $J(\frac{d}{dx}K(x)+\frac{d}{dx}L(x))$, collecting coefficients, and restoring $\frac{\sigma_a\sigma_n}{\sqrt{\sigma_n^2+x^2\sigma_a^2}} \equiv \sigma$ where simplifications are possible gives the final PDF of the truncated RnG random variable.

$$f_v(x) = \frac{1}{e^{\frac{-\alpha^2}{2\sigma_a^2}}-e^{\frac{-\beta^2}{2\sigma_a^2}}}\left[\frac{\sigma_n}{\sqrt{2\pi}(\sigma_n^2+x^2\sigma_a^2)}\left(\alpha e^{\frac{-\alpha^2}{2\sigma^2}}-\beta e^{\frac{-\beta^2}{2\sigma^2}}\right) + \frac{\sigma_a\sigma_n^2}{(\sigma_n^2+x^2\sigma_a^2)^{\frac{3}{2}}}\left[\Phi\left(\frac{\beta}{\sigma}\right)-\Phi\left(\frac{\alpha}{\sigma}\right)\right]\right] \tag{36}$$

C. PDF of v^2 with Truncation

With $Y = v^2$, find $P(Y \le y)$, or $F_Y(y)$. Since v^2 is non-negative, $F_Y(y) = 0$, for $y < 0$. $F_Y(y) = P(Y \le y) = P(-\sqrt{y} \le v \le \sqrt{y}) = F_v(\sqrt{y}) - F_v(-\sqrt{y})$, for $y > 0$.

$$f_Y(y) = \frac{d}{dy}F_v(\sqrt{y})-\frac{d}{dy}F_v(-\sqrt{y}) \tag{37}$$

$$= \frac{f_v(\sqrt{y})+f_v(-\sqrt{y})}{2\sqrt{y}} \tag{38}$$

Substituting $f_v(x)$ from Eq. 36,

$$f_Y(y) = \frac{1}{2\sqrt{y}}\cdot\frac{1}{e^{\frac{-\alpha^2}{2\sigma_a^2}}-e^{\frac{-\beta^2}{2\sigma_a^2}}} \cdot\left[\frac{\sigma_n}{\sqrt{2\pi}(\sigma_n^2+(\sqrt{y})^2\sigma_a^2)}\left(\alpha e^{\frac{-\alpha^2}{2\sigma^2}}-\beta e^{\frac{-\beta^2}{2\sigma^2}}\right) + \frac{\sigma_a\sigma_n^2}{(\sigma_n^2+(\sqrt{y})^2\sigma_a^2)^{\frac{3}{2}}}\left[\Phi\left(\frac{\beta}{\sigma}\right)-\Phi\left(\frac{\alpha}{\sigma}\right)\right]\right] + \frac{1}{2\sqrt{y}}\cdot\frac{1}{e^{\frac{-\alpha^2}{2\sigma_a^2}}-e^{\frac{-\beta^2}{2\sigma_a^2}}} \cdot\left[\frac{\sigma_n}{\sqrt{2\pi}(\sigma_n^2+(-\sqrt{y})^2\sigma_a^2)}\left(\alpha e^{\frac{-\alpha^2}{2\sigma^2}}-\beta e^{\frac{-\beta^2}{2\sigma^2}}\right) + \frac{\sigma_a\sigma_n^2}{(\sigma_n^2+(-\sqrt{y})^2\sigma_a^2)^{\frac{3}{2}}}\left[\Phi\left(\frac{\beta}{\sigma}\right)-\Phi\left(\frac{\alpha}{\sigma}\right)\right]\right] \tag{39, 40}$$

Restoring v^2, x, and gathering terms results in the PDF of v^2 with truncation.

$$f_{v^2}(x) = \frac{1}{|x|}\cdot\frac{1}{e^{\frac{-\alpha^2}{2\sigma_a^2}}-e^{\frac{-\beta^2}{2\sigma_a^2}}} \cdot\left[\frac{\sigma_n}{\sqrt{2\pi}(\sigma_n^2+x^2\sigma_a^2)}\left(\alpha e^{\frac{-\alpha^2}{2\sigma^2}}-\beta e^{\frac{-\beta^2}{2\sigma^2}}\right) + \frac{\sigma_a\sigma_n^2}{(\sigma_n^2+x^2\sigma_a^2)^{\frac{3}{2}}}\left[\Phi\left(\frac{\beta}{\sigma}\right)-\Phi\left(\frac{\alpha}{\sigma}\right)\right]\right] \tag{41}$$

REFERENCES

[1] A. Ballew, A. Kuzmanovic, and C.C. Lee, "Fusion of live audio recordings for blind noise reduction," in *Information Fusion (FUSION)*. ISIF, July 2011.

[2] D.G. Brennan, "Linear diversity combining techniques," *Proc. of the IEEE*, vol. 91, no. 2, pp. 331 – 356, Feb 2003.

[3] R.H. Clarke, "A statistical theory of mobile radio reception," in *Bell Systems Technical Journal*, 1968.

[4] B. Sklar, "Rayleigh fading channels in mobile digital communication systems. i. characterization," *Communications Magazine, IEEE*, vol. 35, no. 9, pp. 136 –146, sep 1997.

[5] R Deepa, Dr K Baskaran, P Unnikrishnan, and A Kumar, "Study of spatial diversity schemes in multiple antenna systems," *Journal of Theoretical and Applied Information Technology*, pp. 619–624, 2009.

[6] J. Winters, "Optimum combining in digital mobile radio with cochannel interference," *Selected Areas in Communications, IEEE Journal on*, vol. 2, no. 4, pp. 528 –539, july 1984.

[7] A. Grant, "Rayleigh fading multi-antenna channels," *EURASIP J. Appl. Signal Process.*, pp. 316–329, Mar. 2002.

[8] M.T. Ivrlac and J.A. Nossek, "Diversity and correlation in rayleigh fading mimo channels," in *Vehicular Technology Conference*, may-1 june 2005, vol. 1, pp. 151 – 155.

[9] A. Paier, T. Zemen, J. Karedal, N. Czink, C. Dumard, F. Tufvesson, C.F. Mecklenbrauker, and A.F. Molisch, "Spatial diversity and spatial correlation evaluation of measured vehicle-to-vehicle radio channels at 5.2 ghz," in *Digital Signal Processing Workshop and 5th IEEE Signal Processing Education Workshop*, jan. 2009, pp. 326 –330.

[10] M. Abramowitz and I. A. Stegun, *Handbook of mathematical functions with formulas, graphs, and mathematical tables*, vol. 55 of *NBS Applied Mathematics Series*, Dover, Washington, D.C., 1964.

[11] W. Kaplan, *Advanced Calculus, 4th Ed.*, Addison-Wesley, Reading MA, 1992.